Rare Metal Materials and Engineering
Volume 55, Issue 4, April 2026
Available online at www.rmme.ac.cn

Science Press

Cite this article as: Shang Jinjin, Yang Hui, Bai Huiwen, et al. Effect of Channel Segregation on Microstructure and Mechanical Properties of Ti45Nb Alloy Wire[J]. Rare Metal Materials and Engineering, 2026, 55(04): 869-876. DOI: https://doi.org/10.12442/j.issn.1002-185X.20250443.

ARTICLE

Effect of Channel Segregation on Microstructure and Mechanical Properties of Ti45Nb Alloy Wire

Shang Jinjin[1,2], Yang Hui[2], Bai Huiwen[2], Wu Yulun[2], Zhao Xiaohua[1,2], Lei Qiang[1,2], He Tao[2], Liu Xianghong[3], Zeng Weidong[1]

[1] State Key Laboratory of Solidification Processing, Northwestern Polytechnical University, Xi'an 710072, China; [2] Western Superconducting Technologies Co., Ltd, Xi'an 710018, China; [3] Northwest Institute for Nonferrous Metal Research, Xi'an 710016, China

Abstract: The effects of channel segregation on the macro- and micro-scale chemical composition, microstructure, hardness, and tensile deformation behavior of Ti45Nb wires were investigated. The results show that wires with severe channel segregation exhibit a macroscopic chemical composition identical to those without segregation, and 3D X-ray imaging result also reveals no abnormalities. After annealing, both types of wires exhibit an equiaxed single-phase microstructure with comparable grain sizes, suggesting that channel segregation has negligible influence on the macroscopic composition and grain size. Metallographic examination reveals that channel segregation manifests as spot-like features in the transverse section and band-like structures in the longitudinal section. EDS analysis identifies these regions as Ti-enriched segregations, with a Ti content higher than that of the surrounding matrix by approximately 4.42wt%. Compared to segregation-free wires, those containing extensive channel segregation demonstrate a 15.5% increase in ultimate tensile strength and a 12.3% increase in yield strength, but suffer a reduction in elongation and reduction of area by 19.8% and 18.9%, respectively. Furthermore, the mechanical properties of wires with segregation show significant fluctuations. Fractographic analysis reveals a larger fracture surface area in segregated wires. Severe dislocation pile-ups occur at the interfaces of these segregated regions, initiating microcrack nucleation. This promotes rapid crack propagation of the Ti45Nb wire, leading to a significant decrease in plasticity and reduction of area.

Key words: Ti45Nb alloy; channel segregation; mechanical properties

1 Introduction

Ti-45wt% Nb alloy is a metastable β-phase titanium alloy with high specific strength, non-magnetism, and excellent high-temperature performance. At 287 °C, it can still retain approximately 60% of its room-temperature strength, and its maximum service temperature is 426 °C. Compared to commercial pure titanium (CP Ti), Ti45Nb alloy exhibits outstanding advantages, such as high strength, high ductility, and relative ease of formability, making it an ideal rivet material for composites and titanium alloys. Consequently, it has completely replaced CP Ti rivets in European and American aerospace applications, demonstrating exceptional comprehensive performance[1–2]. However, a significant challenge arises during the vacuum arc remelting (VAR) process of binary Ti-Nb alloys. The considerable difference in density between titanium (low density) and niobium (high density) combined with inverse segregation (k_{Nb}=1.58) leads to a density inversion between the Ti-enriched mushy zone and the bulk liquid. This density inversion induces vertically upward thermosolutal convection under gravity. If the flow velocity of this convection exceeds the solidification growth rate, local remelting occurs. The increased permeability at these remelted sites further enhances liquid flow, intensifying remelting and ultimately leading to the formation of channel segregation[3–5]. Since X-ray analysis shows dark spot-like features in the transverse section of ingot, this phenomenon is also technically referred to as black spots or freckles. After hot and cold working, freckles in Ti45Nb wire ingots cannot be completely eliminated. These defects are easily visible during

Received date: August 26, 2025
Foundation item: National Natural Science Foundation of China (U24A2038)
Corresponding author: Liu Xianghong, Ph. D., Professor, Northwest Institute for Nonferrous Metal Research, Xi'an 710016, P. R. China, Tel: 0086-29-86514501, E-mail: xhliu@c-wst.com

etching examination, which urgently needs to be addressed.

In reality, the channel segregation has been widely researched in the directional solidification of Al-Cu, Pb-Sn, and Ni-based superalloys systems. Flemings[6] studied the formation of channel segregation in Al-Cu alloy by directional solidification experiments, and found that Al-enriched channel segregation tends to form when the melt flow direction aligns with the solidification growth direction and the flow velocity exceeds the growth rate. Sarazin et al[7] conducted a series of directional solidification experiments on Pb-Sn alloys and demonstrated that Sn content, temperature gradient, and growth rate directly influence channel segregation. Yuan et al[8] employed a coupled cellular automaton-finite difference method to simulate the incubation process of channel segregation during directional solidification of Pb-Sn alloys, achieving the first microscopic-scale simulation of channel formation. Liu et al[9] investigated the influence of VAR process parameters on channel segregation in NbTi alloys, showing that optimized VAR parameters can mitigate channel segregation in large-scale industrial ingots. Zhang et al[10] investigated the causes of wire breakage in NbTi superconducting wires and found that Ti-rich defects are a significant cause of breakage in these wires. Furthermore, Ren et al[11] established a three-dimensional Eulerian two-phase model to study the evolution of channel segregation in directionally solidified nickel-based single-crystal superalloy CMSX-4, revealed that weaker transverse heat flow can suppress the formation of channel segregation. Ref. [12 – 15] reported that once channel segregation forms in superalloys or Nb47Ti alloys, it is difficult to eliminate during subsequent processing and heat treatment, which adversely affects the mechanical properties of the final product. Han[16] investigated that channel segregation in single-crystal superalloys leads to a decrease in high-temperature and medium-temperature creep-rupture performance. Shu et al[17] studied the influence of freckles on the creep-rupture performance of large-scale UGTC47 directionally solidified blades for heavy-duty gas turbines. They found that freckle defects can alter the fracture mechanism of material from micro-void coalescence fracture to intergranular fracture. The extensive eutectic phases and carbides enriched along grain boundaries promote the initiation of voids and cracks, which significantly degrades the stress rupture performance of the blades.

While previous research on Ti45Nb alloy has primarily focused on the effects of heat treatment and processing techniques on its microstructure and mechanical properties[18–22], few studies have examined the influence of channel segregation on the microstructure and mechanical performance of rivet wires. In the present study, composition and microstructure of channel segregation in Ti45Nb wires were researched under both macroscopic and microscopic views. A comparative analysis was conducted to investigate the effects of channel segregation on the mechanical properties of the wires, thereby providing theoretical support for the process design and optimization of continuous cold heading of Ti45Nb alloy wires. This finding not only provides a theoretical basis for optimizing the application standards of Ti45Nb wire, but also significantly contributes to the quality improvement of Ti45Nb wire products.

2 Experiment

Two Ti45Nb alloy ingots with diameter of 520 mm were fabricated by traditional process (referred to as TP) and high homogeneity process (referred to as HP) using an industrial-scale VAR furnace, separately. A comparison of the corresponding process parameters is provided in Table 1. The ingots were subsequently processed through forging, rolling, vacuum annealing, and cold drawing to produce cold-processed wires with a diameter of 5.0 mm for fastener applications. The Nb and O were analyzed using a Thermo iCAP7000 inductively coupled plasmaatomic emission spectrometer (ICP-AES) and an LECO ONH836 series elemental analyzer. After annealing the cold-processed wire in vacuum heat treatment furnace at 830 °C for 1 h[19], the surface processing layer of the samples was removed by grinding with sandpaper, followed by vibratory polishing with SiO_2 suspension to achieve a mirror finish. Subsequently, the samples were etched using a mixed solution of HCl and HNO_3 in a volume ratio of 7∶3 to obtain metallographic samples for microstructural observation and energy dispersive spectroscope (EDS) analysis. Specifically, microstructural characterization and microchemical analysis were performed using an Olympus GX71 optical microscope (OM) and a JSM-IT800 scanning electron microscope (SEM). A METROTOM 1500 industrial CT was employed for three-dimensional X-ray analysis. Room-temperature mechanical tests were conducted using an Instron 5982 universal testing machine, with a pre-yield strain rate of 7×10^{-5} s^{-1} and a post-yield crosshead speed of 5 mm/min. The Vickers hardness was analyzed using ZHVμ-A micro-Vickers hardness tester, with square pyramid diamond indenter, a load of approximately 3 N, and holding for 10 s. Finally, dislocation arrangements and pile-up degrees at the interfaces of segregated regions were characterized by scanning transmission electron microscope (TEM, FEI Talos F200X). In addition, TEM thin foils were prepared using a focused ion beam (FIB, FEI Helios G4).

Table 1 Comparison of process parameters between TP and HP

Parameter	TP	HP
Current/kA	16	16
Voltage/V	39	39
Number of melting cycle	3	3
Cooling method	Water cooling	Water cooling combined with helium cooling

3 Results and Discussion

3.1 Macroscopic composition of wires

TP and HP samples were taken from Ti45Nb wires for chemical composition analysis. The results show that the Nb and O contents in TP and HP samples meet the standard requirements, with comparable average composition and good macroscopic compositional homogeneity. Detailed results are presented in Table 2.

Randomly selected wire segments with the length of 50 mm from both TP and HP samples were subjected to three-dimensional X-ray analysis. No obvious macroscopic segregation is observed in either TP or HP wires, as shown in Fig.1.

Based on macroscopic composition and three-dimensional X-ray analyses, both TP and HP wires exhibit comparable Nb and O contents as well as composition homogeneity.

3.2 Microstructure and microcomposition

Fig. 2 shows OM images of the transverse sections of TP and HP wires. After annealing, both the wires exhibit equiaxed microstructure with comparable grain sizes. According to the ASTM E112 standard, the grain size of both wires is rated as Grade 6. However, there are differences. TP wire contains a large number of spot-like features with a size of approximately 15 μm, which appear both at grain boundaries and within grain interiors, with a small amount of intergranular characteristic. In addition, a clustered dark-colored region with a diameter of about 650 μm can be observed in the central area of TP wire.

Table 2 Nb and O contents of TP and HP wires (wt%)

Sample	Nb	O
TP 1#	45.69	0.074
TP 2#	45.69	0.075
TP 3#	45.62	0.074
HP 1#	45.54	0.077
HP 2#	45.41	0.081
HP 3#	45.50	0.076

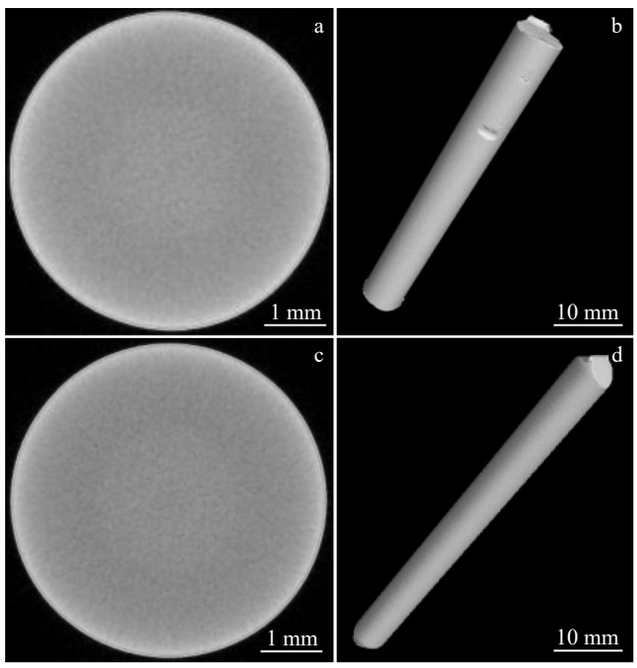

Fig.1 Three-dimensional X-ray inspection results of Ti45Nb wires: (a−b) TP wire; (c−d) HP wire

Fig. 3 presents OM images of the longitudinal sections of TP and HP wires. The annealed wires produced by both processes also exhibit equiaxed microstructures along the longitudinal direction with comparable grain sizes. The distinct difference lies in TP wire, where a significant number

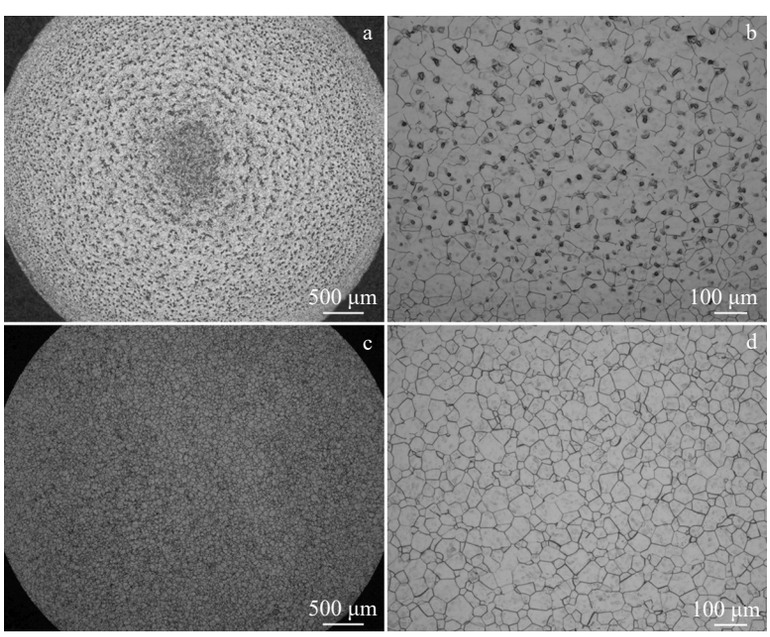

Fig.2 OM images of transverse sections of Ti45Nb wires: (a−b) TP wire; (c−d) HP wire

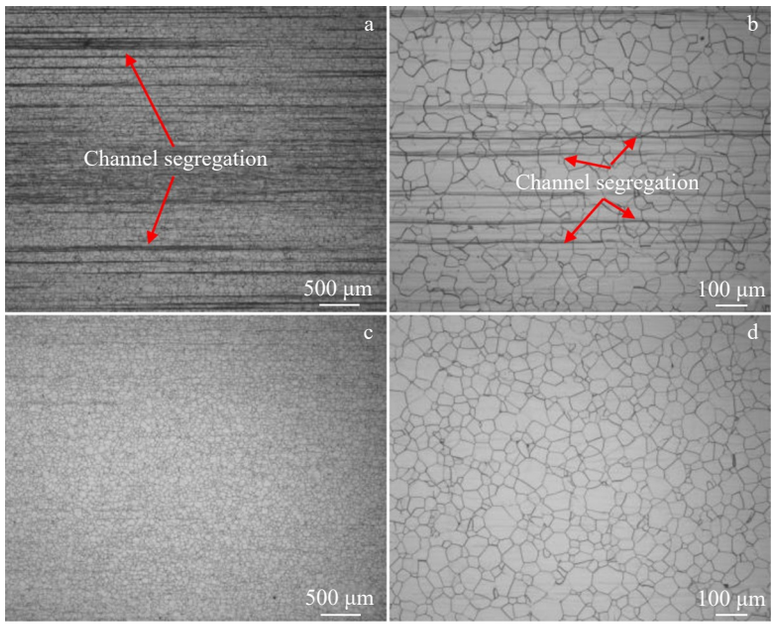

Fig.3 OM images of longitudinal sections of Ti45Nb wires: (a−b) TP wire; (c−d) HP wire

of banded structures aligned parallel to the processing direction are observed in the longitudinal section. These features exhibit characteristic lengths measured in centimeters.

Fig. 4 presents EDS elemental mapping results of the transverse sections of TP and HP wires. The results reveal that the spot-like features observed in OM images, which appear as banded structures in the longitudinal direction, correspond to Ti-enriched regions.

Fig. 5 presents EDS elemental mapping results of the longitudinal sections of TP and HP wires, and Fig. 6 shows EDS line scanning profiles of TP wire. These analyses confirm that the banded structures are Ti-enriched regions, with approximately 15 μm in width, distributed along the longitudinal direction in a roughly parallel but non-equidistant pattern.

Furthermore, EDS point scanning analysis reveals that the Ti content in these segregation regions is 4.42wt% higher than that of the matrix, as shown in Table 3.

In general, based on the analysis of the microstructure and composition of the transverse and longitudinal sections of the TP and HP wires, it is demonstrated that the TP wires contain numerous Ti-enriched segregation regions. These regions appear as spot-like features in the transverse direction and banded structures in the longitudinal direction. They are distributed throughout nearly the entire cross-section of the

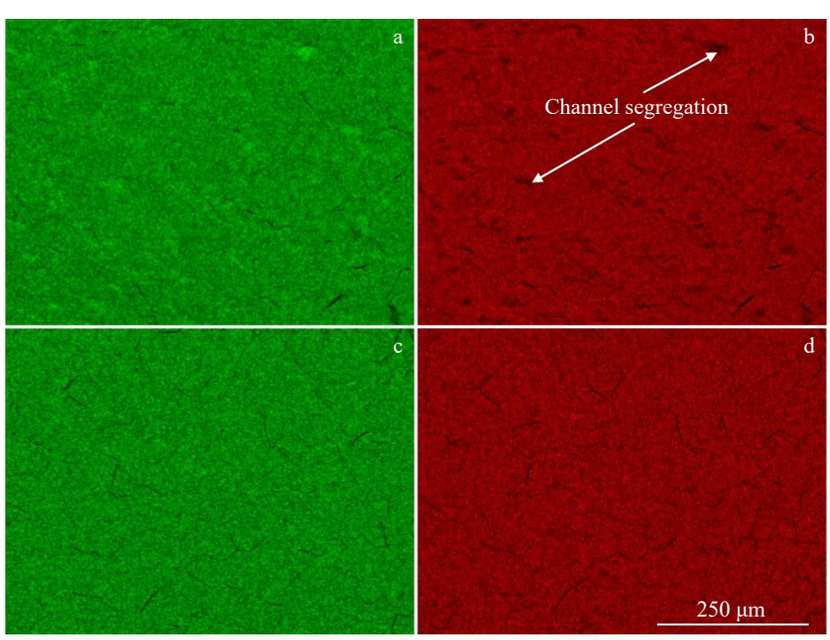

Fig.4 EDS element mappings of transverse sections of Ti45Nb wires: (a−b) TP wire; (c−d) HP wire

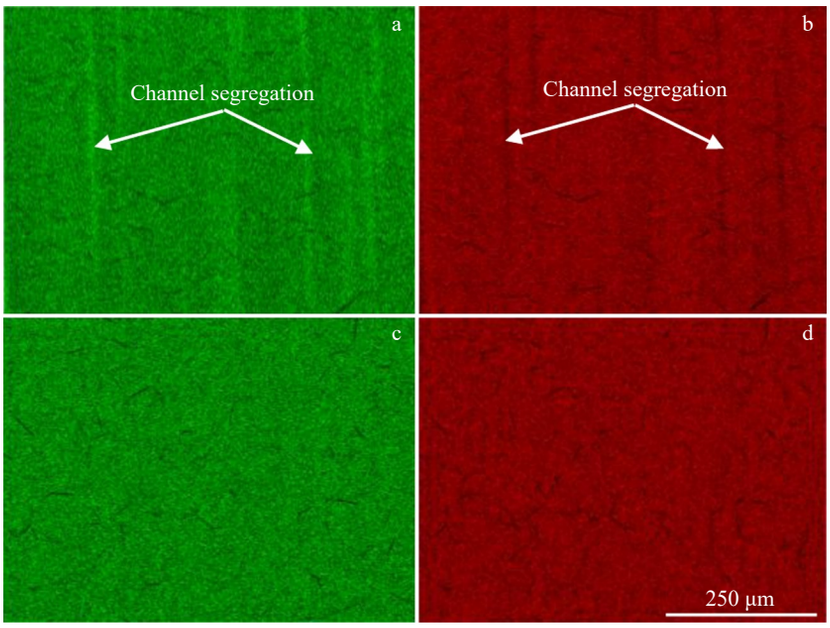

Fig.5 EDS element mappings of longitudinal sections of Ti45Nb wires: (a−b) TP wire; (c−d) HP wire

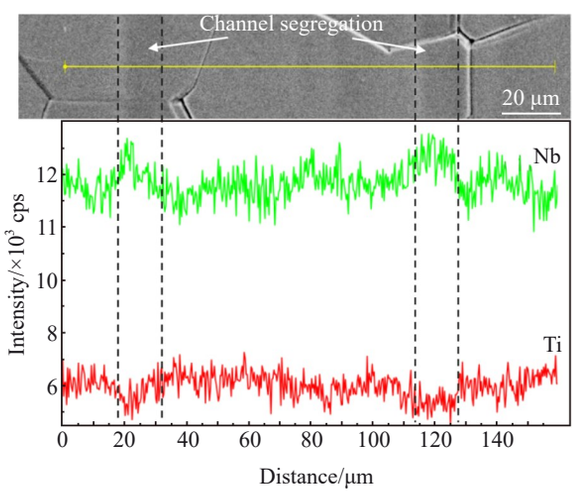

Fig.6 EDS line scanning results of longitudinal section of TP wire

Table 3 EDS point scanning results of channel segregation region and matrix of TP wire (wt%)

Region	Ti	Nb
Channel segregation	59.57	40.43
Matrix	55.15	44.85

wire, with a diameter of approximately 15 μm and lengths measured in centimeters. The Ti content in these regions is about 4.42wt% higher than that of the matrix. This compositional deviation aligns with the characteristics of channel segregation in Ti45Nb alloys.

3.3 Vickers hardness

Microhardness tests were conducted on both TP and HP wires, and the results are presented in Table 4. As shown in Table 4, the average Vickers hardness value from five measurement points on TP wire is 180 HV, with a coefficient of variation (C_V) of 8.35%. In comparison, HP wire shows an average Vickers hardness of 163 HV with a significantly lower C_V of 2.84%. The Vickers hardness of the TP wire is slightly higher than that of the HP wire, and the degree of hardness fluctuation in TP wire is also greater than that in HP wire, exhibiting more significant inhomogeneity. Such inhomogeneity may lead to a reduction in deformation compatibility during material processing. Furthermore, the effective transfer of applied loads during mechanical testing may be impeded due to microstructure and hardness variations, potentially resulting in uneven material flow and reduced plasticity.

Table 4 Vickers hardness of channel segregation region and matrix under load of approximately 3 N (HV)

Point	1	2	3	4	5	Average
TP	169	204	167	169	192	180
HP	164	159	156	168	167	163

3.4 Mechanical properties

In accordance with the requirements of AMS 4928D standard, 10 sets of macroscopic tensile property analyses were conducted on TP and HP wires. The results are summarized in Fig. 7. TP wire with substantial channel segregation exhibits 15.5% higher ultimate tensile strength (R_m) and 12.3% higher yield strength ($R_{p0.2}$) compared to those of segregation-free wire. However, its elongation (A) and reduction of area (Z) are 19.8% and 18.9% lower than those of segregation-free wire, respectively. Furthermore, analysis of the performance variability in both types of wires shows that C_V values of R_m, $R_{p0.2}$, A, and Z for TP wires are 4.37%, 3.50%, 14.58%, and 10.70%, respectively. In contrast, the C_V values of R_m, $R_{p0.2}$, A, and Z for HP wires are 1.02%, 1.91%, 3.56%, and 3.58%, respectively. These results clearly demonstrate that the performance stability of TP wires is significantly inferior

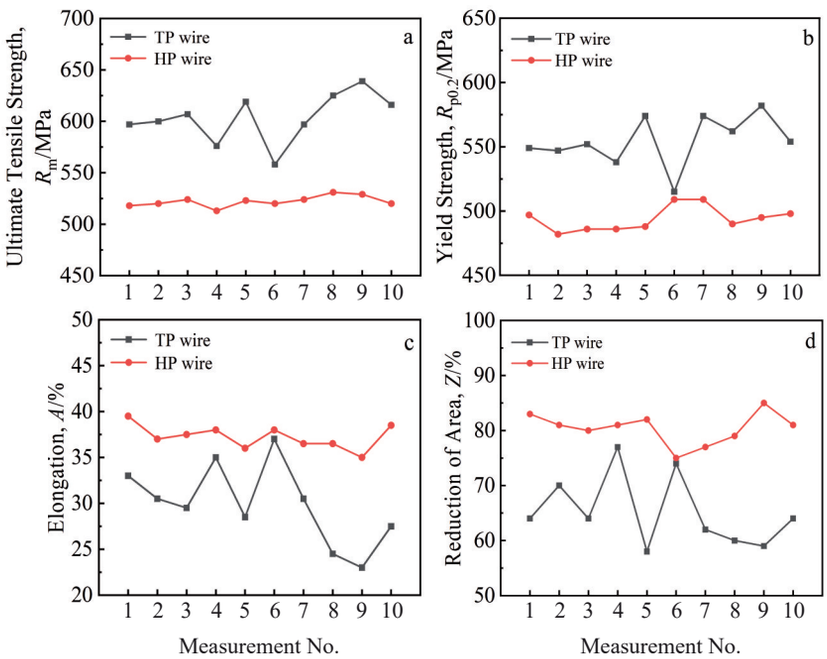

Fig.7 Comparison of tensile properties between TP and HP wires: (a) ultimate tensile strength; (b) yield strength; (c) elongation; (d) reduction of area

to that of HP wires.

Overall, the wire containing channel segregation generally exhibits higher strength, lower plasticity, and greater performance variability. These characteristics are detrimental to continuous cold heading for rivet manufacturing, potentially leading to issues such as rivet deformation incompatibility and cracking.

A comparative analysis was conducted on the tensile fracture morphologies of Ti45Nb wires with and without channel segregation. The fracture cross-sectional area of the segregation-free wire is approximately 2.8 mm^2 (Fig. 8a), exhibiting typical ductile fracture characteristics with macroscopic necking and uniformly distributed deep dimples at the microscopic level (Fig. 8b). In contrast, the fracture cross-sectional area of the wire with channel segregation reaches about 3.5 mm^2 (Fig. 8c), and its cleavage region is significantly larger than that of the segregation-free sample, indicating a distinct tendency toward brittle fracture.

Further observation reveals that although the dimple sizes are similar in both types of fractures, the dimpled regions of the sample with channel segregation contain numerous Ti-enriched voids (Fig. 8d). The Ti content in these voids is approximately 4.21wt% higher than that of the matrix, consistent with the composition of channel segregation regions mentioned earlier. It can be inferred that the significant compositional difference between the channel segregation region and the matrix strongly impedes dislocation motion during deformation, leading to severe dislocation pile-ups at the interface of the segregation region. The high stress concentration generated at the tip of these pile-ups readily induces microcracks. These microcracks are propagated rapidly, ultimately resulting in macroscopic brittle

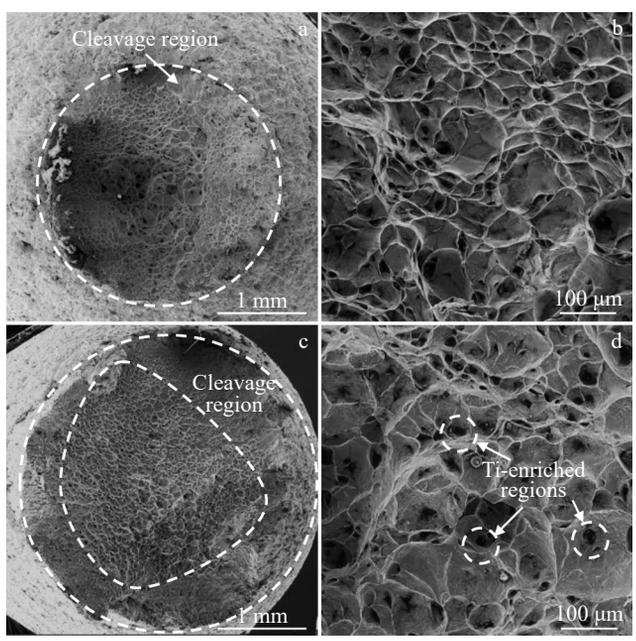

Fig.8 Tensile fracture morphologies of HP wire (a – b) and TP wire (c–d)

fracture characteristics and significantly reducing the plasticity and reduction of area of the Ti45Nb wire.

TEM thin foils at dimples were prepared by FIB technique with corresponding selected area electron diffraction (SAED) pattern and EDS results shown in Fig. 9. Bright-field images reveal that there is no obvious interface between channel segregation and the matrix, but severe dislocation pile-ups are observed, with slight dislocation slip at the segregated sites (Fig. 9a). The diffraction pattern indicates that this region

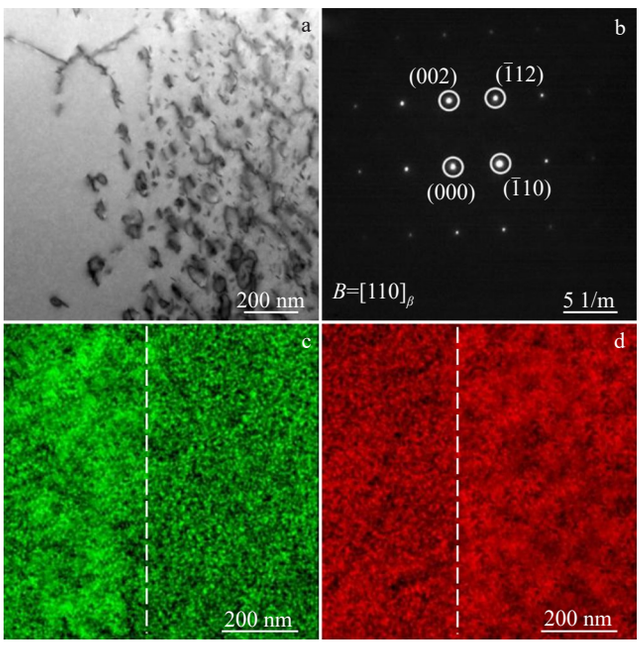

Fig.9 TEM bright-field image (a), corresponding SAED pattern (b), and EDS elemental distribution maps for Ti (c) and Nb (d) of channel segregation region

consists of a single β phase (Fig. 9b). In addition, elemental analysis of this region confirms that the channel segregation sites are rich in Ti and insufficient in Nb (Fig. 9c and 9d). Collectively, these results demonstrate that the compositional gradient between the segregation region and the matrix leads to dislocation pile-ups, subsequently promoting microcrack initiation and propagation.

4 Conclusions

1) The Ti45Nb wires prepared by the two VAR processes (TP and HP) exhibit consistent macroscopic chemical composition of elements, such as Nb and O, and no obvious segregation is detected by three-dimensional X-ray analysis.

2) OM observation reveals that both TP and HP wires display single-phase equiaxed microstructures after annealing, with similar grain sizes corresponding to ASTM Grade 6. The distinctive feature is the presence of numerous spot-like features in transverse sections and banded structures in longitudinal sections of TP wire. EDS analysis confirms that these abnormal structures are Ti-enriched segregation, whose Ti content is higher than that of the matrix by approximately 4.42wt%, exhibiting characteristic of typical channel segregation.

3) Macroscopic tensile testing demonstrates that wires with substantial channel segregation exhibit 15.5% higher ultimate tensile strength and 12.3% higher yield strength, but 19.8% lower elongation and 18.9% lower reduction of area compared to those of segregation-free wires. Fracture analysis shows that the wire with channel segregation has a larger fracture cross-sectional area and displays a distinct tendency toward brittle fracture. The primary mechanism is determined to be severe dislocation pile-ups at segregation region interfaces due to significant compositional differences between segregation regions and the matrix. These compositional differences readily initiate the microcracks, which are propagated rapidly, ultimately leading to substantial degradation in plasticity and reduction of area.

References

1 Zhao Qingyun, Xu Feng. *The Chinese Journal of Nonferrous Metals*[J], 2010, 20(1): 1021 (in Chinese)

2 Zhang Lijun, Wang Xingyun, Guo Qiyi *et al*. *Aeronautical Manufacturing Technology*[J], 2013, 16: 129 (in Chinese)

3 Fu Baoquan, Zhang Pingxiang, Li Jinshan *et al*. *Rare Metal Materials and Engineering*[J], 2014, 43(11): 2702 (in Chinese)

4 Fu Baoquan, Zhang Pingxiang, Li Jinshan *et al*. *Rare Metal Materials and Engineering*[J], 2014, 43(12): 3143 (in Chinese)

5 Shang J J, He Y S, Yang C *et al*. *The 14th World Conference on Titanium (Ti 2019)*[C], Paris: EDP Sciences, 2020: 1

6 Flemings M C. *ISIJ International*[J], 2000, 40(9): 833

7 Sarazin J R, Hellawell A. *Metallurgical Transactions A*[J], 1988, 19(7): 1861

8 Yuan L, Lee P D. *Acta Materialia*[J], 2012, 60(12): 4917

9 Liu Xianghong, Shang Jinjin, Wu Yulun *et al*. *Journal of Materials Research and Technology*[J], 2023, 27(1): 5029

10 Zhang Z Y, Matsumoto S, Choi S *et al*. *Physica C: Superconductivity*[J], 2011, 471(21–22): 1547

11 Ren N, Li J, Panwisawas C *et al*. *Acta Materialia*[J], 2021, 206: 1

12 Wang Z C, Li J R, Liu S Z *et al*. *Rare Metal Materials and Engineering*[J], 2022, 51(10): 3533

13 Li T, Shen H F. *Rare Metal Materials and Engineering*[J], 2022, 51(11): 4076

14 Zhu B H, Chen Z Z, Cao Y F *et al*. *Materials*[J], 2021, 14(4): 1

15 Liu Y, Wang F, Ma D X *et al*. *Acta Materialia*[J], 2024, 266: 1

16 Han Dongyu. *Formation and Evolution of Freckle Defect and Its Effect on Creep Rupture Properties of Ni-based Single Crystal Superalloys*[D]. Hefei: University of Science and Technology of China, 2021 (in Chinese)

17 Shu Guogang, Xuan Weidong, Yu Xu *et al*. *Rare Metal Materials and Engineering*[J], 2025, 54(8): 1997 (in Chinese)

18 Genereux P D, Borg C A. *Superalloys 2000*[C]. Warrendale: TMS, 2000: 19

19 Liang S J, Hou F Q, Li Y H *et al*. *Rare Metal Materials and Engineering*[J], 2015, 44(9): 2203

20 Völker B, Jäger N, Calinb M *et al*. *Materials and Design*[J], 2017, 114: 40

21 Gai Yongchao, Zhang Rui, Zhou Zijian *et al*. *Rare Metal Materials and Engineering*[J], 2024, 53(1): 159 (in Chinese)

22 Wang X X, Qi Z C, Chen W L. *Materials Science & Engineering A*[J], 2021, 813: 1

通道偏析对Ti45Nb合金丝材组织及力学性能的影响

尚金金[1,2]，杨　辉[2]，白惠文[2]，吴与伦[2]，赵小花[1,2]，雷　强[1,2]，何　涛[2]，刘向宏[3]，曾卫东[1]

(1. 西北工业大学 凝固技术国家重点实验室，陕西 西安 710072)

(2. 西部超导材料科技股份有限公司，陕西 西安 710018)

(3. 西北有色金属研究院，陕西 西安 710016)

摘　要：研究了通道偏析对Ti45Nb合金丝材宏观/微观化学成分、显微组织、硬度及拉伸变形行为的影响。结果表明，存在大量通道偏析的丝材，其宏观化学成分与无偏析丝材一致，三维X射线成像也未发现异常。退火后，2类丝材均呈现等轴单相组织，晶粒尺寸相近，表明通道偏析对宏观成分及晶粒尺寸无明显影响。金相组织显示通道偏析在丝材横截面呈现为斑点状组织；纵截面呈现为条带状结构。能谱分析显示通道偏析为富Ti偏析，其Ti含量较基体高出约4.42wt%。与无偏析丝材相比，存在大量通道偏析的丝材抗拉伸强度和屈服强度分别高了15.5%和12.3%，但延伸率和断面收缩率分别低了19.8%和18.9%，且存在通道偏析的丝材性能波动大。断口分析显示，存在通道偏析丝材断口截面面积大，位错在偏析区界面处严重塞积，诱发了微裂纹形核，促使裂纹源快速扩展，导致材料塑性及断面收缩率显著下降。

关键词：Ti45Nb合金；通道偏析；力学性能

作者简介：尚金金，男，1984年生，博士，正高级工程师，西部超导材料科技股份有限公司，陕西 西安 710018，电话：029-86514504，E-mail：sjandsj@c-wst.com